The Surface Properties of a van der Waals Fluid*

Nicolas G. Hadjiconstantinou
Lawrence Livermore National Laboratory
Livermore, CA 94551

Alejandro L. Garcia †
Center for Computational Sciences and Engineering
Lawrence Berkeley National Laboratory
Berkeley, California 94720

and

Berni J. Alder
Lawrence Livermore National Laboratory
Livermore, CA 94551

April 28, 1999

Abstract

Surface properties are obtained from an extension of the direct simulation Monte Carlo algorithm to a hard sphere system with an infinite range, weak attractive potential that obeys the van der Waals equation of state. Liquid-vapor surface tension measurements both

*Submitted to

†Permanent address: Physics Dept., San Jose State University, San Jose, Calf. 95192

with and without a gravitational field are in agreement with experimental values for simple substances. These measurements are also consistent with the van der Waals theory using the measured interface density profile though the theory does not explicitly account for the work required to form the density gradient in the interface for the reference hard sphere system.

The mean field van der Waals (vdW) model has been popular because it is simple enough to be rigorously derivable from statistical mechanics, yet realistic enough to capture both the liquid and vapor states of matter, as well as predict the coexistence region by the use of the Maxwell construction. However, theoretical studies have so far been unable to predict rigorously the surface properties of the vdW model without resorting to approximations. Surface tension theories [1] require either information about the density gradient through the liquid-vapor interface or knowledge of the radial distribution function in that region. For the vdW model this information cannot be obtained experimentally since real fluids only approximately correspond to this model. Numerically, a vdW fluid is difficult to simulate rigorously by molecular dynamics because the particle interaction consists of a hard sphere repulsion with a weak, long ranged attraction [2]. Recently it was shown that the Direct Simulation Monte Carlo (DSMC) procedure can be generalized to the simulation of dense hard sphere systems [3], which in turn can further be extended to the simulation of the van der Waals equation of state [4]. It has thus become possible for the first time to obtain the density profile through the interface and the surface tension of a true vdW fluid and to compare these measurements with theoretical predictions.

For completeness, the simulation algorithm is outlined briefly. For details on DSMC, see [5, 6]; extensions to higher densities are described in [3, 4, 7]. The fluid is represented as a collection of particles, specified by their positions, $\{\mathbf{r}_i\}$, and velocities, $\{\mathbf{v}_i\}$. At each time step, these particles are sorted into spatial cells; the dimensions of a cell are a fraction of a mean free path [8]. The number of collisions that occur within a cell during a time step τ is computed from the hard sphere collision rate, $\Gamma = \Gamma_B(n,T)Y(n)$, where n is the number density, T is the temperature, Γ_B is the Boltzmann (i.e., dilute gas) collision rate and Y is the Enskog factor that rigorously gives the collision rate in a dense gas [9]. For the simulations presented here τ is one-tenth of the mean free time. Random collision partners are selected within a cell given the hard sphere collision probability $\mathcal{P}(\mathbf{v}_i, \mathbf{v}_j) = |\mathbf{v}_r| / \sum_{i,j} |\mathbf{v}_r|$, where $\mathbf{v}_r = \mathbf{v}_i - \mathbf{v}_j$ and the sum is over elligible partners. The post-collision velocities, $\mathbf{v}'_i$ and $\mathbf{v}'_j$, conserve momentum and energy. The post-collision relative velocity is chosen statistically as $\mathbf{v}'_r = |\mathbf{v}_r|\hat{R}$ where $\hat{R}$ is a unit vector with random direction, uniformly distributed on the unit sphere.

In order to obtain the vdW equation of state, each pair of colliding particles is assigned a displacement $\mathbf{d}$ that combines a hard sphere excluded volume and a long range weak attractive force. Specifically,

$$\mathbf{d}_i = \frac{\mathbf{v}'_r - \mathbf{v}_r}{|\mathbf{v}'_r - \mathbf{v}_r|}\left(\sigma - \frac{a\sigma}{b_2 YkT}\right); \qquad \mathbf{d}_j = -\mathbf{d}_i, \tag{1}$$

where k is Boltzmann's constant, a is the van der Waals attraction coefficient, $b_2 = \frac{2}{3}\pi\sigma^3$, and σ is the hard sphere diameter. For the results presented here $m = k = \sigma = a = 1$. After all collisions have been processed, each particle is moved ballistically so $\mathbf{r}_i(t+\tau) = \mathbf{r}_i(t) + \mathbf{v}_i(t)\tau + \frac{1}{2}\mathbf{a}\tau^2 + \mathbf{d}_i$ and $\mathbf{v}_i(t+\tau) = \mathbf{v}_i(t) + \mathbf{a}\tau$ where $\mathbf{a}$ is the acceleration of an applied, external field (e.g., gravity), when present.

The collision process outlined above results in a virial that leads to the van der Waals equation of state [9]

$$P = nkT\left(1 + b_2 nY(n) - \frac{an}{kT}\right). \tag{2}$$

If in the calculation of Y and d the mean density is used in each cell then (2) is exactly reproduced [4], however, at densities in the vdW loop region only the homogeneous state is found since the displacement is independent of density fluctuations. Similarly, the vdW equation of state with a Maxwell tie line can be generated and again no two phase region is observed since there is no compensating free energy gain to offset the cost of forming the inhomogeneity associated with the interface surface.

To generate coexisting phases at different densities requires having Γ and d evaluated using the local density. This, however, for reasons that are not entirely understood, seems to lead to a nonlinear coupling between the displacement and the collision rate through the density fluctuations, which leads to an unphysical correlation that manifests itself as a stratification of the density aligned with the collision cells. This correlation results in a discrepancy between the correct equation of state, eq. (2), and the measured equation of state. Unfortunately, although this discrepancy is small when compared to the absolute value of the pressure, it is of the same order as the capillarity generated pressure differences at liquid-vapor coexistence. To break up this artificial correlation an additional displacement of σ in a random direction is given to each colliding particle. This random displacement modifies the transport properties but its only effect on the equation of state is to reduce the discrepancy caused by the anomalous correlation [7]. The introduction of this random displacement, however, has the effect of smearing the fluid vapor-liquid interface, and leads to the largest source of uncertainty in the results presented below.

Simulations initially at a density in the two phase region evolve to form drops at the correct tie-line liquid density, n_ℓ, with the remainder of the material at the saturated vapor density, n_v. However an initially uniform density distribution does not phase separate into drops and vapor during reasonable running times unless an initial high density region is present to nucleate the phase separation. Dense regions, initially at half the liquid density, have been observed to succesfully evolve to drops; the exact size of the initial state required for nucleation is still under investigation. Fig. 1 shows the coagulation and relaxation of two proto-droplets into the equilibrium circular configuration. In this constant temperature simulation ($T/T_c = 0.756$, where T_c is the critical temperature) the initial density is 0.48 within the droplets and 0.10 elsewhere. The final densities inside and outside the drop are very nearly the equilibrium coexistence liquid and vapor densities of $n_\ell = 0.63$ and $n_v = 0.03$.

The surface tension of the circular drops is calculated using the Laplace equation (in two dimensions)

$$P_d = P_\infty + \frac{\gamma}{R}, \tag{3}$$

where P_d is the pressure in the interior of the drop and P_∞ is the pressure in the ambient vapor far away from the drop. The temperature is held fixed by use of a thermostat in which particle velocities are adjusted locally. The system is equilibrated for at least 5000 collision times (usually 9000) before statistical samples are gathered. The size of the simulation domain in the x and y directions is 54.6 σ and contains 4×10^5 particles. The drops are between 20σ and 30σ in diameter.

The radially symmetric pressure is calculated as the flux of normal momentum through small test areas. Typical pressure and density profiles are shown in Fig. 2. In this figure the vdW loop is evident from the variation in pressure through the interface. The definition of an equimolar radius [1]

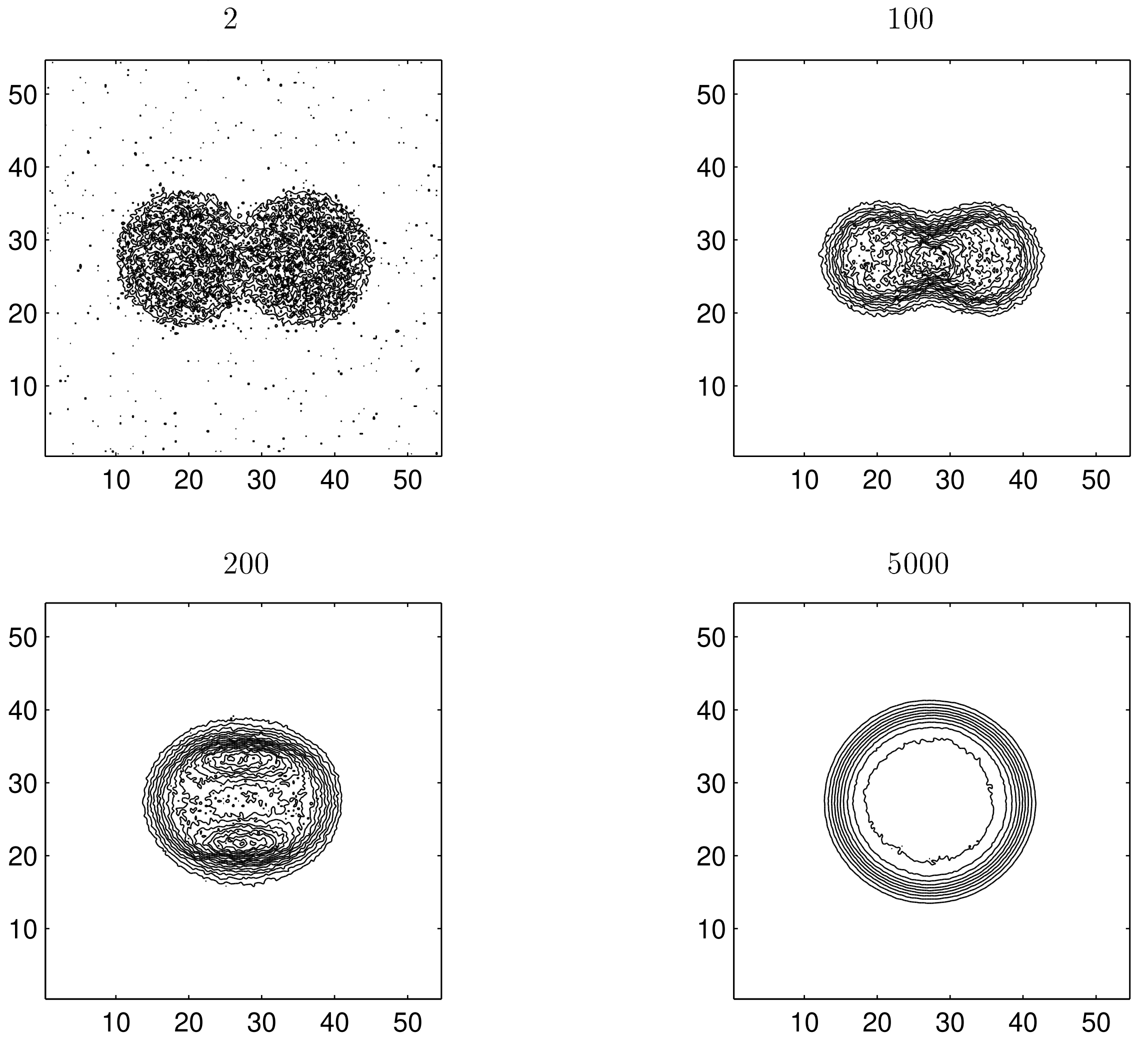

Figure 1: Snapshots of the time evolution of two proto-droplets in a vapor bath to a circular drop. The system is contained in a rectangular shaped box of dimensions $54.6\sigma \times 54.6\sigma \times 2.7\sigma$ with 4×10^5 particles. Density contours are shown starting $n = 0.05$ in increments of 0.1; succesive snapshots are taken at 2, 100, 300, and 5000 collision times.

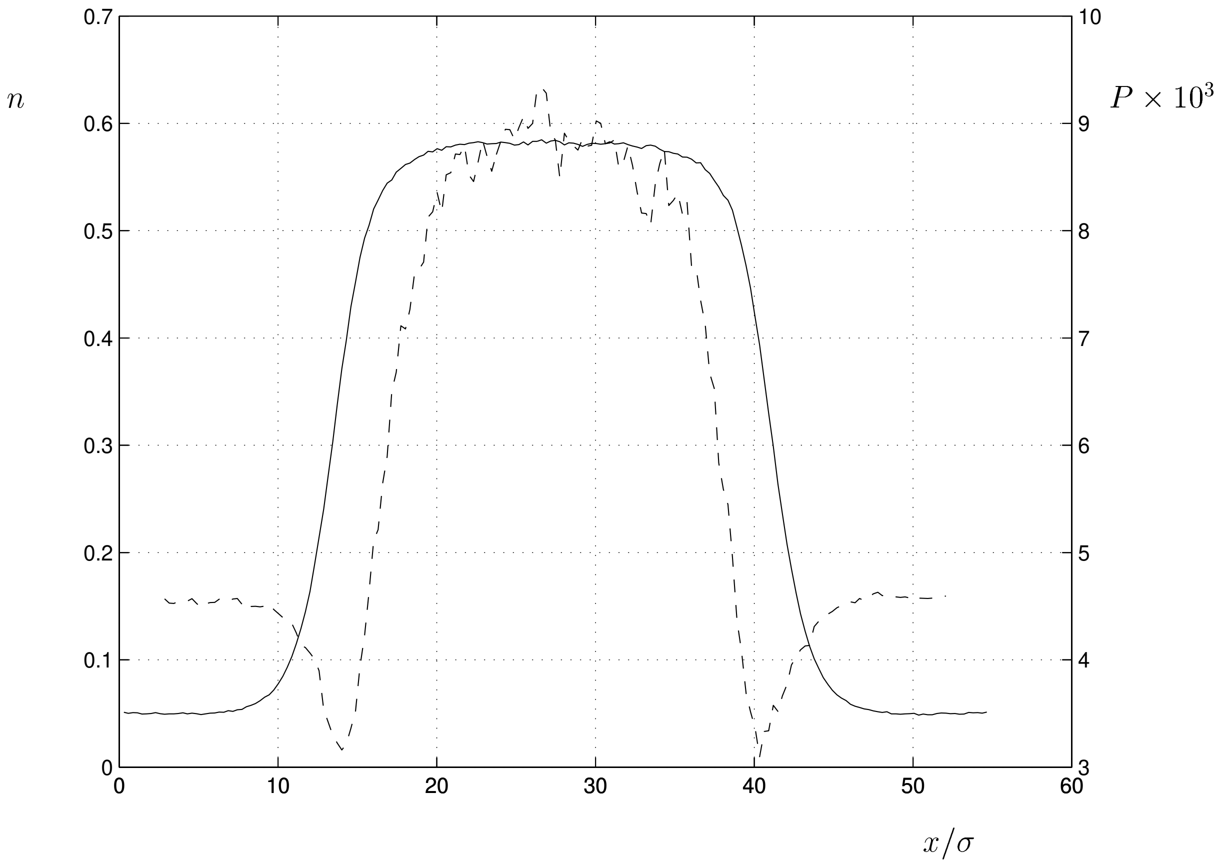

Figure 2: Density (solid line) and pressure (dashed line), in reduced units, across a system of total width 54.6σ held at $T/T_c = 0.8$.

(modified for two dimensions)

$$r_e{}^2 = \frac{1}{n_\ell - n_v} \int_0^\infty r^2 \frac{dn}{dr} dr \quad (4)$$

can be shown to be approximately equivalent to the radius at which the density reaches the value $n(R) = n_v + 0.4(n_\ell - n_v)$; this definition of the drop radius R has been subsequently used. The surface thickness, δ, has been defined as

$$\delta = -(n_\ell - n_v)\left[\frac{dr}{dn}\right]_{r=R} . \quad (5)$$

The values of δ, R, and γ are given in Table 1. The drops are large enough that Tolman size corrections due to surface curvature are smaller than the simulation error bars [10]. The curvature also leads to an increase in the vapor pressure by a factor of $e^{\gamma/nmRkT}$, as predicted by the Kelvin equation [1]. This effect is always less than 15% and hence it was not explicitly accounted for, but rather included in the error estimates. The main sources of error are the fairly sluggish equilibration dynamics close to the equilibrium coexistence densities and the error associated with the random displacement.

An independent estimate of the surface tension, which confirms the results presented above, was obtained from its mechanical definition. Previous studies have shown that a constant external body force, such as gravity, facilitates the phase separation into liquid and vapor for a fluid in the two-phase region [4]. When a spatially varying gravitational field is introduced the liquid-vapor interface becomes curved and from this curvature the surface tension can be measured. One of the simplest ways to achieve this is spinning the fluid in a gravitational field. A variant that makes the computations significantly more tractable is to introduce a lateral "centrifugal" acceleration that is a linear function of the distance from the center of the simulation box (at $x = 0$), that is, $a_x = \omega^2 x$. This external field, in conjunction with a constant gravitational field ($a_y = -g$) in the vertical (y-direction), reproduces solid body rotation in a two-dimensional configuration. The simulations presented here are three-dimensional but shallow in the z-direction, which results in significant computational savings. The fluid reaches hydrostatic equilibrium in this field while the temperature is held fixed by use of a thermostat.

The simulations have been limited to one temperature close to the critical point because at lower temperatures n_ℓ/n_g increases and the computational

T/T_c	R	δ	$\gamma_L \times 10^2$	$\gamma_e \times 10^2$	$\gamma_{vdW} \times 10^2$
0.889	12 ± 1	7.5 ± 0.6	1.1 ± 0.5	2.4	2 ± 0.5
0.844	13.5 ± 1	6 ± 0.6	3.1 ± 0.4	3.9	3.1 ± 0.8
0.800	14 ± 1	5 ± 0.6	5.6 ± 1	5.6	$4.4\pm 1.$
0.756	11.5 ± 1	5 ± 0.6	8.9 ± 1.5	7.5	6.6 ± 1
0.756	14.5 ± 1	4.5 ± 0.6	9.4 ± 1.5	7.5	5.9 ± 1
0.711	11.5 ± 1	4.5 ± 0.6	12.5 ± 3	9.4	8.7 ± 1
0.711	15 ± 1	4 ± 0.6	12.5 ± 3	9.4	7.8 ± 1

Table 1: Surface tension as a function of temperature computed from the Laplace equation (γ_L), from Elsner's method (γ_e), and the vdW theory (γ_{vdW}). The interface thickness (δ), and drop radius (R) are also shown.

cost increases substantially. This is mainly due to the fact that in order for stochastic particle simulations to maintain statistical accuracy the minimum number of particles in any cell must not be appreciably less than twenty. The higher density ratios require a higher total number of molecules since density in the gaseous phase decreases exponentially with height.

Fig. 3 shows a typical density profile from the simulations. The surface tension is calculated by applying momentum conservation in the y-direction on the control volume shown in the same figure. By momentum balance,

$$2\gamma \cos\theta = \int_1 P dA + \int \rho g dV - \int_2 P dA, \tag{6}$$

where the pressure integrals are over the top and bottom faces of the control volume. Each term on the r.h.s., as well as the interface angle θ, can be evaluated from the simulation data. Note that to avoid edge effects, the control volume is constructed such that its sides are sufficiently far away from the specular walls bounding the fluid. Faces 1 and 2 are placed optimally such that the area integrals in (6) are as accurate as possible. The interface angle θ tends toward a preferred "contact" angle between wall, liquid and vapor and since this contact angle is not known *a priori* for this system, the sides of the control volume are placed away from the sides of the simulation box as far as is practical while maintaining a control volume sufficiently large. In the simulation the pressure integrals are evaluated by measuring the net momentum transfer through faces 1 and 2.

The surface tension obtained through this method depends on the magnitude of the applied gravity as given by the Bond number, defined as $Bo = m\bar{n}g\delta^2/\gamma$, where $\bar{n}$ is the mean simulation density. For $Bo \geq 1$, it appears that gravity has an effect on the surface tension of the interface and the interface thickness. Unfortunately, the accuracy of the results for $Bo \geq 1$ is insufficient to allow any firm conclusions to be drawn: compressibility effects become important, and the relative importance of the left hand side of equation (6) with respect to the right hand side decreases proportionally to Bo making the results susceptible to significant error. Table 2 shows that interface thickness and surface tension are consistent with the droplet simulation results when $Bo \ll 1$.

The above simulation measurements are first of all compared to a simple model of surface tension that summarizes experimental observations. An empirical method for evaluating the surface free energy, ϕ, is integrating the Helmholtz free energy per particle, f, across the tie line between the volumes

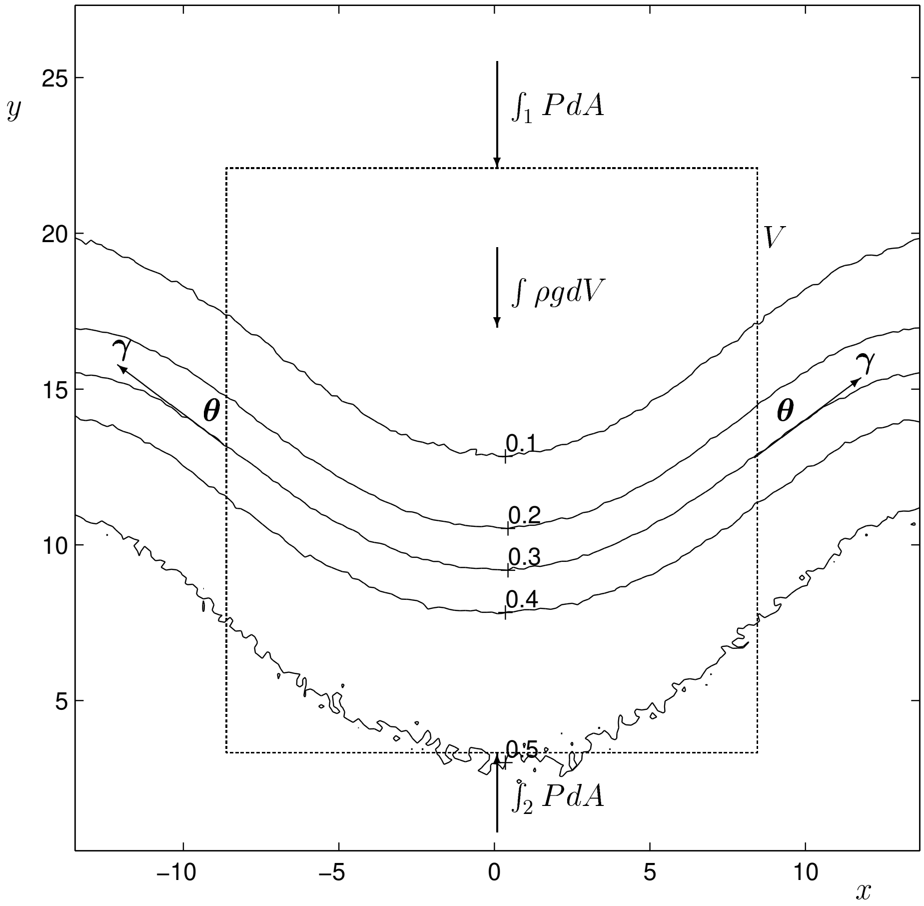

Figure 3: Number density versus position at $T/T_c = 0.89$ for $g = 2.82 \times 10^{-4}$ and $\omega = \sqrt{4g}$. Surface tension angle, θ, is obtained from the $n = 0.3$ contour; the control volume is outlined by the dashed rectangle. The simulation box measures 27.3 σ in both the x and y-directions and contains 4×10^5 particles.

$g \times 10^3$	Bo	δ	$\gamma \times 10^2$	θ
14	$5.5 \pm 1.$	4 ± 0.4	3.1 ± 0.6	50^o
5.6	3.4 ± 0.6	5 ± 0.5	2.6 ± 0.5	57^o
2.8	2.1 ± 0.5	5.5 ± 0.5	1.9 ± 0.5	63^o
0.7	0.66 ± 0.25	7 ± 0.5	1.2 ± 0.4	66^o
0.28	0.35 ± 0.2	7.2 ± 0.5	1.3 ± 0.3	70^o
0	0	7.5 ± 0.6	1.1 ± 0.5	–

Table 2: Surface tension and surface thickness computed from surface curvature for $T/T_c = 0.89$. The effective rotation rate is $\omega = \sqrt{4g}$. The value for $g = 0$ is from Table 1.

of the two coexisting phases [11],

$$\phi = \frac{1}{3}\alpha(T)\int_{v_g(T)}^{v_\ell(T)} \frac{\mu - pv}{v^{5/3}} dv \tag{7}$$

where v is the inverse number density and μ is the chemical potential. The coefficient $\alpha(T)$ effectively acts as a Jacobian relating the integration in length to the integration in volume, that is, $r = \alpha v^{1/3}$. This approach has been found to fit the data for simple substances with $\alpha \approx 0.6$ [11] at all temperatures.

The surface tension is then obtained from the thermodynamic relation,

$$\gamma_e(T) = T\int_T^{T_c} \frac{\phi(T)}{T^2} dT. \tag{8}$$

Taking $\alpha(T) = 0.6$, the values of surface tension are listed in Table 1 and found to be in good agreement with the surface tension measured from the droplet pressure. This indicates that the vdW model gives a reasonable surface tension for simple substances.

Next the results are compared to the celebrated van der Waals theory of surface tension. The surface tension is given by [1]

$$\gamma_{vdW} = \int_0^\infty \left\{ F(n) + \frac{1}{2} m \left(\frac{dn}{dr} \right)^2 \right\} dr, \tag{9}$$

where $F(n)$ is the Gibbs free energy excess per unit volume as obtained from the difference between the chemical potential of the coexisting phases at temperature T, $\mu(T) = \mu_\ell(T) = \mu_v(T)$, and $M(n,T)$, the chemical potential within the vdW loop,

$$F(n) = \int_{n_\ell}^{n} [M(n,T) - \mu(T)] dn, \tag{10}$$

with $F(n_\ell) = F(n_v) = 0$. This theory has not been tested with the vdW equation of state since it requires knowledge of the density gradient through the interface and the coefficient m, which is discussed below.

Estimates of the surface tension can be obtained (see Table 1) by utilizing the measured density gradient through the interface and exploiting the fact that the free energy reaches a minimum when the two terms in eq. (9) contribute equally [1], which leads to:

$$\gamma_{vdW} = \int_{n_v}^{n_\ell} 2 \frac{F(n)}{dn/dr} dn \approx \frac{2\delta}{n_\ell - n_v} \int_{n_v}^{n_\ell} F(n) dn. \tag{11}$$

The last numerical approximation is sufficiently precise in view of the substantial uncertainty in the numerical simulation. The agreement between the vdW theory and the simulation results suggests that the vdW surface tension model is of greater generality than its derivation indicates. As expected, the theory and data are in better agreement near the critical point than at lower temperatures indicating that the Taylor expansion to second order in gradient used in eq. 9 gives a more accurate approximation when the density gradient is smaller.

When the equation of state (2) is replaced with an equation of state that has a flat tie-line (instead of a vdW loop) [4], no phase separation occurs. In this homogeneous system the surface tension is zero since $F(n) = 0$. Thus in a gravity simulation ($g = 2.8 \times 10^3$) where the fluid is forced to segregate into liquid and vapor regions to satisfy the hydrostatic condition, the surface tension is zero (-0.5 ± 0.5 from eq. (6) with $\theta = 55^o$) to within the accuracy of the simulations.

An approximate value for m can be calculated using the simulation data by rewriting eq. (9) as $m \approx \gamma_{vdW}\delta/(n_\ell - n_v)^2$ and a temperature independent value of $m = 0.8 \pm 0.2$ is obtained. This result is to be contrasted with the theoretical prediction [1] that m is the second moment of the interaction potential $\Psi(r)$,

$$m = -\frac{1}{6}\int r^2 \Psi(r) d^3r. \tag{12}$$

This second moment diverges for long ranged interaction potentials. Moreover, even the general expression, which is Taylor expanded [1] to give eq. (12), diverges. From the formulation of the mean field model the contribution to m from the constant long range potential should vanish since all the particles interact, independent of their position, so the formation of the gradient requires no work. However, this term does not explicitly account for the work required to rearrange the reference hard sphere system to form the relatively steep density gradient, a quantity that can be obtained by molecular dynamics simulation [12].

The interface thickness is observed to be a monotonically increasing function of temperature and independent of the computational domain size, within statistical error bars, when the domain size is doubled. Additionally, the interface thickness reported here is consistent with the results of molecular dynamics simulations for 3-5 times smaller systems using the short-ranged Lennard-Jones potential. The long range potential of the vdW model has the effect of damping out capillary waves and possibly any associated divergence in the thickness [14]. If any divergences in the thickness due to to the long range potential itself are present they were not observed in the numerical experiments [13].

Further work involves the removal of the random displacement to reduce the uncertainties in the measurements, and the evaluation of m from molecular dynamics simulations. The simulation method presented here can also be used to generate the time evolution of droplet dynamics, such as droplet formation and coagulation, and these phenomena are being investigated in more detail.

The authors wish to thank F. Alexander, D. Rothman, J. Weeks, and B. Widom for enlightening discussions, and T. Heier and A. Shapiro for help with the computations. This work is sponsored, in part, by the National Science Foundation and by the Department of Energy, contract W-7405-ENG-48.

References

[1] J.S. Rowlinson and B. Widom, *Molecular Theory of Capillarity*, Clarendon, Oxford (1982).

[2] J.L. Lebowitz and O. Penrose, *J. Math. Phys.* **7** 98 (1966).

[3] F.J. Alexander, A.L. Garcia, and B.J. Alder, *Phys. Rev. Lett.* **74** 5212 (1996).

[4] F.J. Alexander, A.L. Garcia, and B.J. Alder, *Physica A* **240** 196 (1997).

[5] G.A. Bird, *Molecular Gas Dynamics*, Clarendon, Oxford (1994).

[6] F.J. Alexander and A.L. Garcia, *Comp. Physics* **11** 588 (1997).

[7] F.J. Alexander, A.L. Garcia, and B.J. Alder, *J. Stat. Phys.* **89** 403 (1997).

[8] F.J. Alexander, A.L. Garcia, and B.J. Alder, *Phys. Fluids* **10** 1540 (1998).

[9] P. Resibois and M. De Leener, *Classical Kinetic Theory of Fluids*, Wiley, New York (1977).

[10] R.C. Tolman, *J. Chem. Phys.*, **17** (1949).

[11] A. Elsner, *Phys. Lett. A* **156** 147 (1991).

[12] D.G. Triezenberg and R. Zwanzig, *Phys. Rev. Lett.* **28** 1183 (1972).

[13] D.E. Sullivan, *Phys. Rev. A* **25** 3 (1982).

[14] J.D. Weeks, D. Bedeaux, and B.J.A. Zielinska, *J. Chem. Phys.* **80** 3790 (1984).